ADVANCING EARTH AND SPACE SCIENCE

Geophysical Research Letters

RESEARCH LETTER

10.1029/2020GL091551

**Key Points:**

- Smoking-gun evidence of pedogenic weathering pyroclastic deposits was found on volcanoes at high elevations
- Our results provide a contextual link between ancient precipitation-driven pedogenic weathering sequences and explosive volcanism on Mars
- Pyroclastics are likely a key component of Mars' sedimentary record, and alteration of these deposits was perhaps a fundamental process on the early Mars

**Supporting Information:**

- Supporting Information S1

**Correspondence to:**

J. R. Michalski
jmichal@hku.hk

**Citation:**

Ye, B., & Michalski, J. R. (2021). Precipitation-driven pedogenic weathering of volcaniclastics on early Mars. *Geophysical Research Letters*, *48*, e2020GL091551. https://doi.org/10.1029/2020GL091551

Received 4 NOV 2020
Accepted 14 JAN 2021



# Precipitation-Driven Pedogenic Weathering of Volcaniclastics on Early Mars

**B. Ye[1,2] and J. R. Michalski[1,2]**

[1]Division of Earth and Planetary Science, University of Hong Kong, Hong Kong, China, [2]Laboratory for Space Research, University of Hong Kong, Hong Kong, China

**Abstract** Compositional stratigraphy, generally composed of Al-rich clay minerals overlying Fe/Mg-rich clay minerals, is observed in many locations on Mars. Here we describe the occurrence of such mineralogical stratigraphy in settings where the protoliths are almost certainly pyroclastic materials. One such example includes altered rocks high on the summit and flanks of explosive volcanoes in Thaumasia Planum. These clay-bearing deposits are most consistent with precipitation-driven weathering of ash deposits. Considering explosive volcanism was pervasive in the Noachian, the early sedimentary record of Mars in some locations is likely dominated by glassy, fragmented, porous, chemically reactive materials with highly specific surface area. These pyroclastic deposits were potentially a critical geological component linking clay minerals to elements of Mars' climate, weathering, and sedimentary puzzle.

**Plain Language Summary** On Earth, basaltic volcanoes are not extremely explosive but on Mars, similar mafic volcanism would have been much more explosive due to lower crustal and atmospheric pressures. Volcanic ash should therefore be extremely widespread on the red planet. In this work, we show a link between the observed clay minerals seen from orbit via visible/near-infrared spectroscopy and a geologic context within ash deposits formed from explosive volcanism. We suggest that the weathering of highly chemically reactive ash deposits can explain the origin of many layered clay-bearing deposits on Mars. Volcanism may have produced ash deposits and driven climate excursions that led to weathering of the ash under somewhat warmer or wetter conditions.

## 1. Introduction

Explosive volcanism is an important geologic process in the Solar System but remains widely underappreciated because it does not produce well defined, mappable lava flows as effusive vents do. But, there are a growing number of studies showing that explosive volcanism likely dominated early episodes of the geologic history of multiple planets (e.g., Bandfield et al., 2013; Gustafson et al., 2012; Kremer et al., 2019; Michalski & Bleacher, 2013; Rogers et al., 2018; Thomas et al., 2014). Violent eruptions would have likely released large quantities of $H_2O$, $SO_x$, $CO_2$, $CH_4$, and $H_2$, and would have resulted in the airfall deposition of vast amounts of fine-grained volcaniclastic materials. Those volcaniclastic materials might have been reworked by wind and water, and would have remained an appreciable fraction of the clastic component of sedimentary rocks on Mars. The erupted greenhouse gasses would have had significant impacts on the early climate (Halevy & Head, 2014; Halevy et al., 2007; Robock, 2000). The interaction between water and these highly chemically reactive glassy fragments could have been common in Mars' early history (Wilson & Head, 1994). In fact, there might have been a coupling between eruption of gases and ash, climate triggers, and aqueous chemical weathering resulting in the widespread occurrence of smectitic clay on Mars (Carter et al., 2013, 2015).

Theoretical studies suggest that basaltic volcanism would have been much more explosive on Mars than it is on Earth, primarily due to the lower gravity and lower crustal pressures on Mars (Wilson & Head, 1994). Indeed, extensive layered, easily eroded, and seemingly fine-grained deposits are found throughout ancient terrains (e.g., the Arabia mantling deposits, Hellas basin floor deposits, the Medusae Fossae Formation, the south polar pitted deposits, the Electris deposits in/around Eridania Basin, and the Argyre basin deposits), which have been suggested by some as potential ash deposits (Grant & Schultz, 1990; Kerber et al., 2012; Moore, 1990). There is little doubt that explosive volcanoes and their associated pyroclastic deposits should have played an important role in shaping the surface of Mars and contributing to the global sedimentary record.

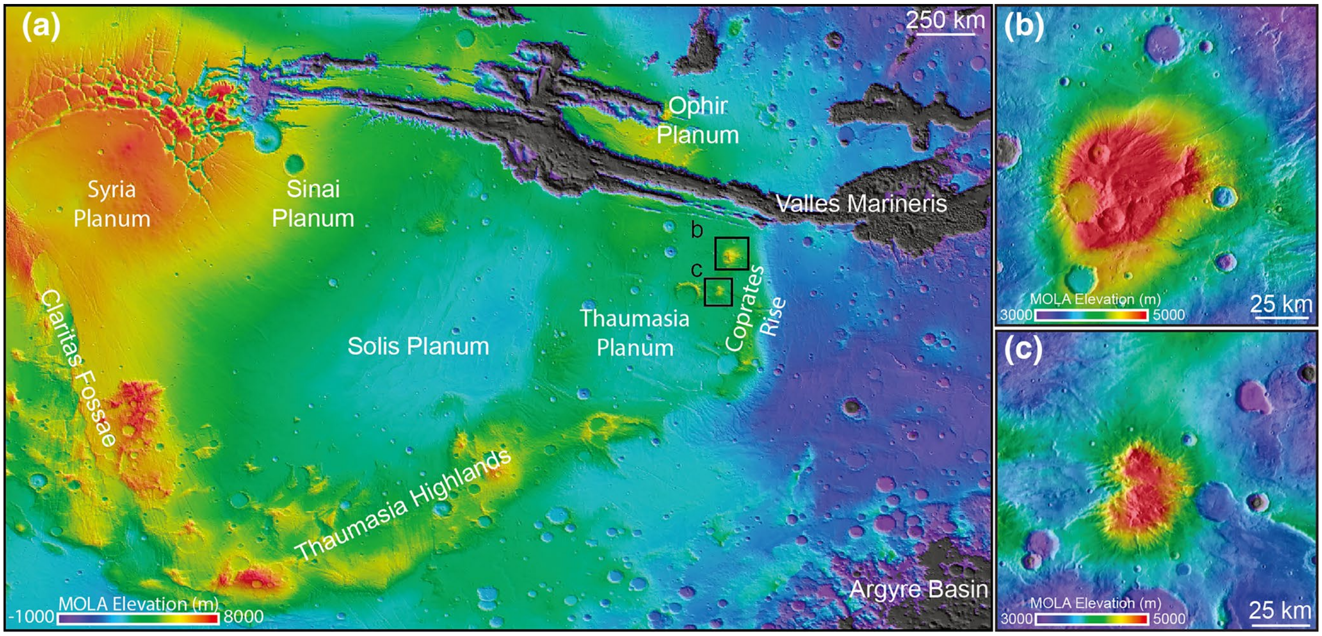


**Figure 1.** (a) The geologic context of the Thaumasia region. MOLA topographic data are draped over MOLA shade-relief data. Two volcanic structures described in the text as "volcano 1" and "volcano 2" are shown in "b" and "c," respectively. MOLA, Mars Orbiter Laser Altimeter.

In this study, we explore the issue of compositional stratigraphy on Mars. It is widely recognized that, in many locations on Mars, Al-rich clay minerals stratigraphically overlie Fe/Mg clay minerals (e.g., Carter et al., 2015). Multiple models exist to explain this observation, but there is a debate with regard to the role of top-down alteration, rainfall versus groundwater, and links to valley networks (J. L. Bishop et al., 2008; Dobrea et al., 2010; Ehlmann et al., 2011; Gaudin et al., 2011). Here we present new evidence that this compositional stratigraphy on Mars formed (1) very early in Mars' history, (2) through top-down alteration driven by precipitation, and (3) within highly chemically reactive volcanic ash. We describe in detail some weathering profiles associated with proposed explosive volcanic edifices in Thaumasia Planum (Figure 1), one of the oldest regions on Mars. This result offers a temporal and contextual link between ancient precipitation-driven pedogenic weathering sequences and explosive volcanism on Mars. Given the likely importance of explosive volcanism in Mars' early history, the alteration of ash deposits was almost certainly a fundamental geologic process and should be considered in more detail when interpreting the stratigraphy and mineralogy of the martian surface.

## 2. Methods

Geomorphological observations of these two volcanos on Thaumasia Planum were made primarily with 6 m/pixel Context Imager (CTX) data (Malin et al., 2007) corrected mosaics (Dickson et al., 2018) and 0.3 m/pixel High Resolution Imaging Science Experiment (HiRISE) data (McEwen et al., 2007). Gridded topographic data from the Mars Orbiter Laser Altimeter and High Resolution Stereo Camera (HRSC) allow quantitative topographic analysis at 463 m/pixel (Smith et al., 2001) and 50 m/pixel, respectively (Neukum et al., 2004). Thermal inertia data derived from the Thermal Emission Spectrometer (TES; Mellon et al., 2000) and the Thermal Emission Imaging System (THEMIS; Christensen et al., 2004; Fergason et al., 2006) were also used to assess thermophysical properties between geologic units.

Surface mineralogy of these two volcanoes was investigated using visible/near-infrared reflectance data from the Compact Reconnaissance Imaging Spectrometer for Mars (CRISM; S. Murchie et al., 2007). We analyzed the 1.0–2.6 μm spectral range of 100 s of CRISM images throughout Mars, but this paper focuses on FRT00023521, FRS0002715F, and FRT00021F18 in detail. Standard data processing procedures were performed to correct for instrument effects, radiometrically calibrate the data and remove most atmospheric effects (e.g., according to Ehlmann et al., 2009 and S. L. Murchie et al., 2009). Standard mineral parameter maps were used to delineate various clay units (Pelkey et al., 2007; Viviano-Beck et al., 2014), and each unit was verified by checking the spectral shapes of I/F data extracted from those units. Average spectra from regions of interest (typically greater than 5 × 5 pixels, at least 3 × 3 pixels) were ratioed to a dusty or spectrally neutral region from the same column of the unprojected image.

## 3. Weathering Sequences on Thaumasia Planum Volcanoes

Two volcanic edifices were identified in Coprates Rise, the east part of Thaumasia Planum. An unnamed feature (referred to here as "volcano 1") is a topographic feature with dimensions 150 km North–South and 90 km West–East located at 300.4°E–18°N (Figure 1b). The structure reaches a maximum height of ∼2 km above surrounding plains and contains a near-circular depression at the summit that is possibly the caldera. Another structure dubbed "volcano 2," located at 299.7°E–20.37°N, reaches 1 km elevation above the surrounding plains and has dimensions 60 km North–South and 30 km West–East (Figure 1c).

These two large putative volcanic structures are dominated by low-thermal inertia materials, and they contain evidence for structural collapse as is seen in some other explosive volcanoes on Mars (Michalski & Bleacher, 2013). Though these structures are interpreted as volcanic features by multiple previous authors (J. Dohm & Tanaka, 1999; Dohm et al., 2001; Xiao et al., 2012), we point out that neither has any associated lava flows and only one of the features has a central collapse pit that would be interpreted as a caldera. The mode slope of the flanks from the caldera rim to basement is about 1.5° and 3° for volcano 1 and volcano 2, respectively. Layered, light-toned materials observed in the summit of volcano 1 at fine scales with CTX data (Figure 2e) might represent pyroclastic deposits. The TES thermal inertia values of the two volcanoes range from ∼180 to 200 J $m^{-2}$ $K^{-1}$ $s^{-0.5}$. The high-resolution thermal inertia derived from THEMIS nighttime temperature data for the two structures ranges from ∼200 to 250 J $m^{-2}$ $K^{-1}$ $s^{-0.5}$, which is relatively low on a global scale and suggests that even the highest inertia areas contain significant fine-grained materials (Fergason et al., 2006). These low thermal inertia materials could be interpreted as ash deposits. As discussed below, the spectral response from the surface is not indicative of dust cover.

These two volcanic structures were modified by erosion and impacts, creating V-shaped valleys (Figures 2 and S1), slumps or landslides, and impact craters. The numerous sinuous channels radiating from the summit are striking features on the flanks of volcano 1 and volcano 2 and are reminiscent of similar patterns on other known volcanoes, such as Alba, Hecates, and Ceraunius (Gulick & Baker, 1990). Channels are typically 1–3 km wide and 10–15 km long, but the maximum length of any channel is ∼90 km. A significant amount of light-toned material is exposed on the floors of the channels (Figures 2c and S3). The light-toned materials usually exhibit small-scale polygonal fractures in HiRISE images (Figures 2f and 2g), similar to desiccation cracks (El-Maarry et al., 2014), which may indicate volume loss in expandable clay minerals (i.e., smectites). Collectively, these two ancient volcanoes on Thaumasia do not look like other effusive volcanoes on Mars, but are morphologically similar to ancient highland paterae (e.g., Hadriaca, Tyrrhena, and Apollinaris Paterae) considered to have explosive volcanic origin (Table S2; Crown & Greeley, 1993). Their response to erosion, lack of lava flows, radiating "V-shaped" channels, low thermal inertia, low topographic relief and slopes are consistent with explosive volcanism.

Previous researchers estimated the absolute model ages for volcano 1 and volcano 2 using crater counting at 4.05 and 3.98 Ga, respectively (Xiao et al., 2012). The best timing constraint however comes from detailed mapping of Tanaka et al. (2014), showing that the interpreted volcanic units are overlain by middle Noachian plains materials (Tanaka et al.'s "middle Noachian highland unit", spanning from 3.84 to 3.95 Ga), meaning these structures are Middle Noachian at youngest and potentially older. In addition, these two volcanoes also show some signatures of remnant crustal magnetization (Connerney et al., 2005; Lillis et al., 2008), suggesting these two volcanoes are pre-Noachian or early Noachian (>4.0 Ga) because the shutdown of the core dynamo and cessation of crustal magnetization occurred around 4.0–4.1 Ga.

A key observation is the identification of compositional stratigraphy within volcanic structures at high (∼2 km) elevation above the surrounding terrain. CRISM images show that the exposures of light-toned materials exhibit distinct spectroscopic signatures consisting of Fe/Mg clay minerals and Al/Si materials (Figure 2c). These light-toned deposits at volcano 1 show a clear vertical stratigraphic relationship; the

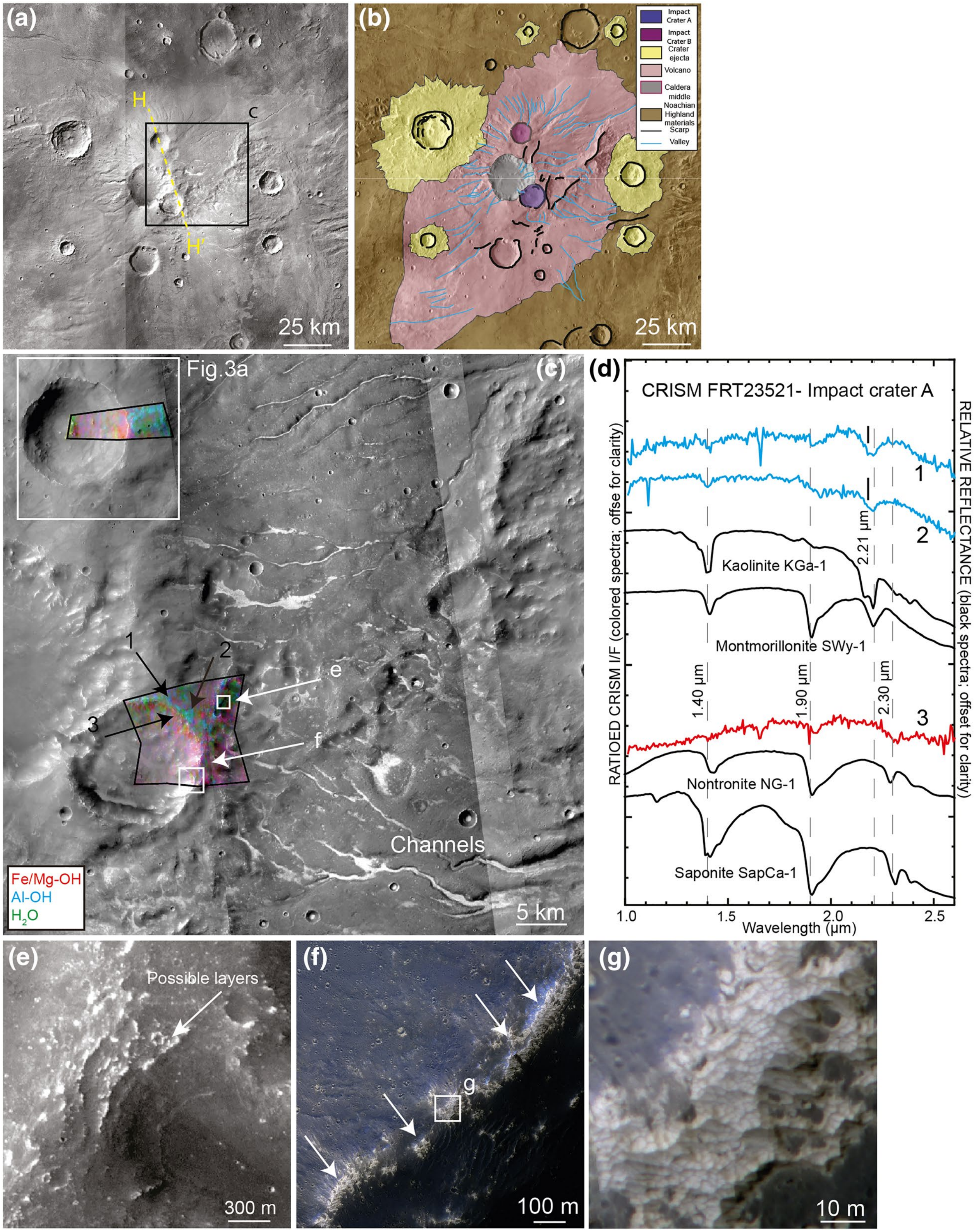
(a)
H
H'
c
25 km
(b)
Impact Crater A
Impact Crater B
Crater ejecta
Volcano
Caldera middle
Noachian Highland materials
Scarp
Valley
25 km
Fig.3a
(c)
1
2
3
e
f
Channels
Fe/Mg-OH
Al-OH
$H_2O$
5 km
(d)
CRISM FRT23521- Impact crater A
1
2
2.21 µm
Kaolinite KGa-1
Montmorillonite SWy-1
1.40 µm
1.90 µm
2.30 µm
3
Nontronite NG-1
Saponite SapCa-1
1.0
1.5
2.0
2.5
Wavelength (µm)
RATIOED CRISM I/F (colored spectra; offse for clarity)
RELATIVE REFLECTANCE (black spectra; offset for clarity)
(e)
Possible layers
300 m
(f)
g
100 m
(g)
10 m

10.1029/2020GL091551

Al/Si materials overlay the Fe/Mg clay minerals (Figures 2c and 3a). Crater B is a ~10 km diameter impact crater in the northern flanks of volcano 1, exhibiting the best exposure in the crater wall (Figures 3a and 3b). The upper Al/Si phase is relatively blue and lower Fe/Mg smectites unit is relative reddish (Figure 3c). The transition of the two colors is gradual and it may indicate the contact between two units is gradational. Volcano 2 contains clay minerals in similar stratigraphic relationships, but the outcrops are not as good due to the lack of exposure created by impact craters (Figure S2). HiRISE images show that this altered material has a smooth surface or exhibits polygonal fractures (e.g., Figure 2g). Based on spectral shapes and band minima observed with CRISM, the Al-rich material is probably kaolinite and possibly allophane or imogolite, and Fe/Mg clay minerals are likely $Mg^{2+}$ or $Fe^{2+}$-rich trioctahedral clays (Figures 2d, 3b, and S2b). Kaolin-group minerals are characterized by a deep, narrow asymmetric doublet absorption near 2.17 and 2.2 μm. Well-crystalline kaolinite has a very sharp, well-defined doublet with two distinct absorptions (Clark et al., 1990). The doublet absorption is not so pronounced in this case and it may indicate the spectra are more consistent with disordered kaolinite, halloysite or kaolinite-smectite mixed-layer clay (Cuadros & Michalski, 2013; Ehlmann et al., 2016; McKeown et al., 2011). The 2.21 μm band minimum and an asymmetry with a shoulder at 2.17 μm strongly indicates kaolin-group minerals are present in some locations.

We note that some Al/Si materials exhibit a broad absorption at 2.19–2.20 μm instead of 2.21 μm (Figure 3b). The 2.21 μm absorption and lack of a doublet are characteristic of an Al smectite phase (e.g., montmorillonite) or an opaline silica phase, with the absorption caused by Al-OH or Si-OH combination stretching and bending vibrations, respectively. The maximum inflection point on the long wavelength side of the 2.2 μm absorption in this setting is 2.34 μm, wider than kaolinite (2.25 μm), and montmorillonite (2.27 μm) but narrower than hydrated silica (2.39 μm). Allophane and imogolite, which are characterized by a broader band centered near 2.19–2.20 μm due to the poorly crystalline Al/Si-OH-bearing units, are most consistent with our observation (J. L. Bishop & Rampe, 2016; J. L. Bishop et al., 2013). The spectra collected from the lower part of the stratigraphy exhibit absorptions centered near 1.40, 1.92, and 2.30 μm, consistent with Fe/Mg smectites (Bishop et al., 2002, 2008) such as Mg-rich or ferrous nontronite (Michalski et al., 2015).

## 4. Discussion

### 4.1. The Origin of the Compositional Stratigraphy

In our study, no candidate hydrothermal or likely diagenetic alteration minerals (e.g., illite, prehnite, and chlorite) were identified. The distribution of hydrous minerals appears extensive and continuous on volcanic edifices at high elevations rather than patchy (Figure 4), which is not consistent with the hydrothermal origin. The clear vertical stratigraphy relationship of clay minerals at volcano 1, consists of a lower Fe/Mg clay unit and an upper Al/Si clay/silica unit, similar to the other compositional stratigraphy observed throughout the southern highland on Mars. Hundreds of examples of compositional stratigraphy have been identified around the global, including within the western Arabia Terra, Valles Marineris, Nili Fossae, Terra Sirenum, Eridania, and Noachis Terra (e.g., Crater et al., 2015; Ehlmann et al., 2011; Le Deit et al., 2012). The widespread distribution points to a significant aspect of the global geologic process. Multiple working hypothesizes were proposed, including top-down leaching, rainfall versus groundwater and links to valley networks (J. L. Bishop et al., 2008; Ehlmann et al., 2011; Gaudin et al., 2011; Michalski et al., 2013; Noe Dobrea et al., 2010). Yet, their origin remains controversial.

**Figure 2.** (a) A CTX mosaic of volcano 1. The black box indicates the location of Figure 2c. The yellow dashed line marks the location of the cross-section profile in Figure 4. (b) A geologic-geomorphic map of volcano 1. (c) CRISM mineral parameter maps (Fe/Mg clay minerals in red, Al/Si materials in blue and hydrous minerals in green) overlaid on CTX images of volcano 1. (d) Ratioed CRISM I/F spectra containing Al/Si materials and Fe/Mg clay minerals from FRT00023521. Library spectra of Al clay minerals and Fe/Mg clay minerals are in black for comparison. Gray lines mark bands near 1.40, 1.90, 2.21, and 2.30 μm. The spectra of kaolinite, montmorillonite, opal, nontronite, and saponite are from the USGS library (Clark et al., 2007). (e) Examples of possible layer outcrop at volcano 1 are shown in the CTX image (K01_053871_1616_XI_18S059W). (f) A subset of color HiRISE image (ESP_026206_1615) shows light-toned materials exposed in crater A, which are clay deposits filled with polygonal fracture as the white arrow indicates. (g) An enlarge figure shows the detail of the polygonal fractures of clay deposits. CRISM, Compact Reconnaissance Imaging Spectrometer for Mars; CTX, Context Imager; HiRISE, High Resolution Imaging Science Experiment.

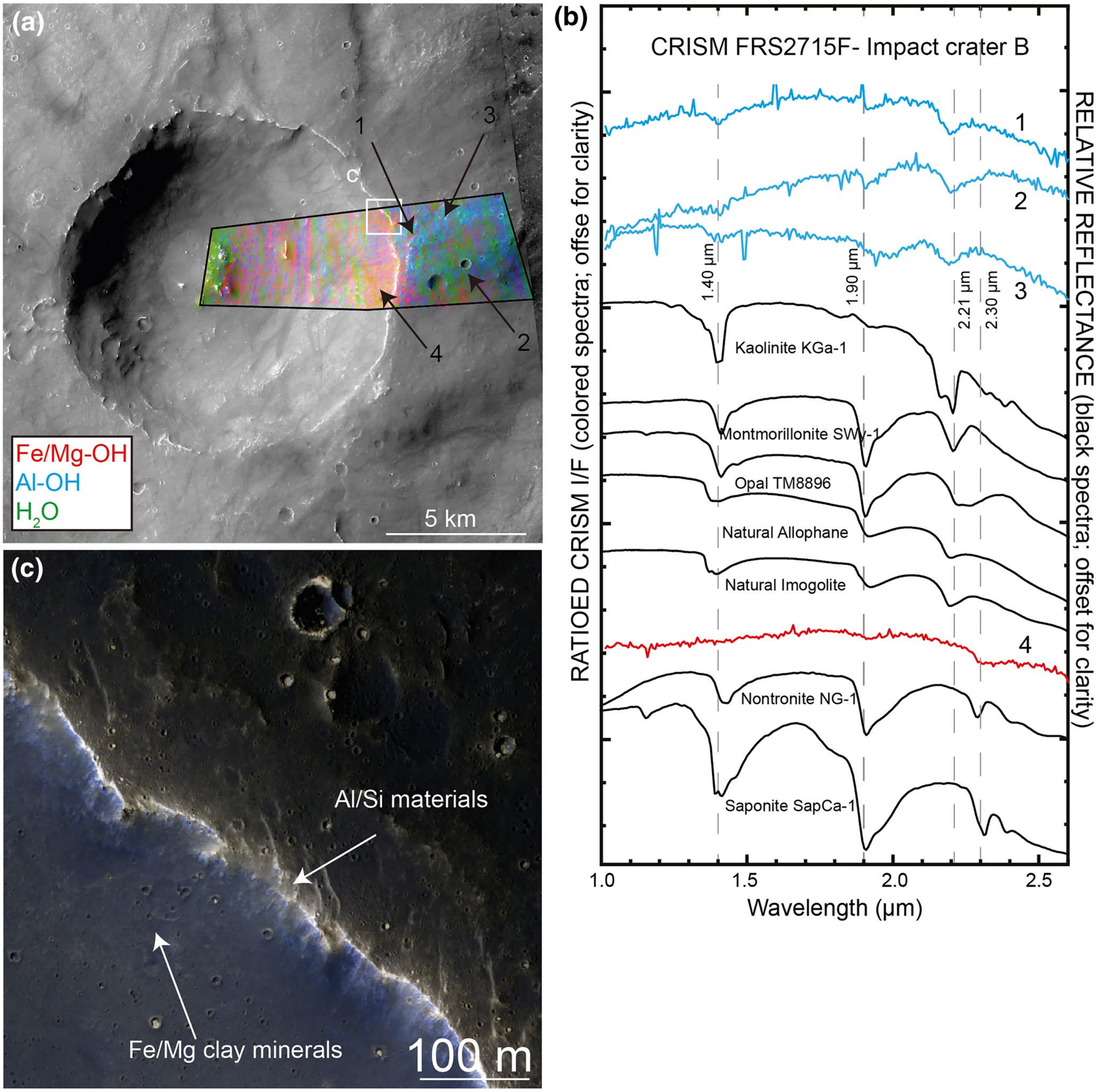


**Figure 3.** (a) Enlarged CRISM mineral parameter map (Fe/Mg clay minerals in red, Al/Si materials in blue and hydrous minerals in green) overlaid on CTX images of volcano 1, showing Al/Si materials stratigraphy overlying Fe/Mg clay minerals. (b) A subset of color HiRISE image (ESP_029450_1620) shows the smooth texture of compositional sequences in the crater wall. (c) Ratioed CRISM I/F spectra contain Al/Si clays and Fe/Mg clays from CRISM FRS0002715F. Library spectra of Al clay minerals, opal and Fe/Mg clay minerals are in black for comparison. Gray lines mark bands near 1.40, 1.90, 2.21, and 2.30 $\mu$m. The spectra of natural allophane and imogolite samples are from J. L. Bishop et al. (2013). The spectra of kaolinite, montmorillonite, opal, nontronite and saponite are from the USGS library (Clark et al., 2007). CRISM, Compact Reconnaissance Imaging Spectrometer for Mars; CTX, Context Imager; HiRISE, High Resolution Imaging Science Experiment.

Our result shows that the compositional stratigraphic relationship is observed at high elevation, on ancient volcanoes, above the surrounding plains. This strongly indicates that, in this setting, the compositional stratigraphy must have formed from chemical weathering of pyroclastic materials driven by rainfall or snowmelt. The elevated setting above the surrounding plains argues against groundwater, which would emerge from depth, and the continuous nature argues against local hydrothermal processes, which would not form

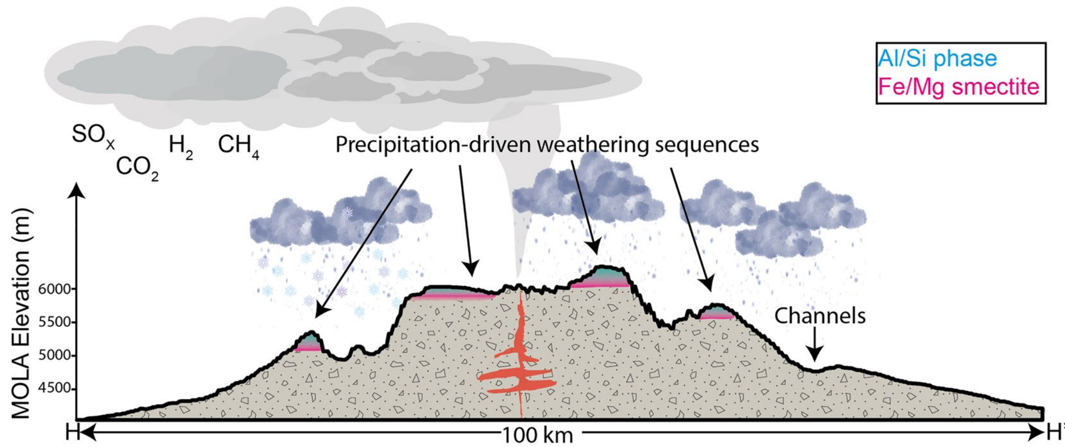


**Figure 4.** A schematic 100 km long cross-section shows an exaggerated MOLA elevation profile of volcano 1 and the location where the alteration is observed (see Figure 2a for context). The weathering sequences (Al/Si phases in blue and Fe/Mg smectite in pink) on the summit and flanks of this volcano must have formed through precipitation, rainfall or snowmelt. Alteration by groundwater is less likely due to the topographic setting. The explosive eruption and others like it elsewhere released a large amount of greenhouse gases over a short period to increase temperature and pressure temporarily, allowing precipitation to occur. The liquid water derived from the snowmelt or rainfall carved fine-grain glassy pyroclastics deposits on the summit and flanks to form channels and compositional stratigraphy rapidly. MOLA, Mars Orbiter Laser Altimeter.

widespread, homogeneous deposits. Allophane and imogolite detected in these two volcano edifices are characteristic of soils formed in tephra or pyroclastic deposits on Earth (Parfitt, 2009; Wada & Wada, 1977). Allophane and imogolite were found within the compositional stratigraphy in Mawrth Vallis, which has been interpreted as evidence for alteration of explosive fragments from nearby supervolcano Eden patera (J. L. Bishop & Rampe, 2016). Indeed, alteration of pyroclastics deposits has been proposed by previous words (McKeown et al., 2009; Wilson & Head, 1994; Wray et al., 2008). Without a clear volcanic context, discriminating volcaniclastic rocks from fluvial/lacustrine/aeolian deposits and impact ejecta at orbital scale remains a great challenge. Our observation of Al/Si phases overlying Fe/Mg smectite on volcanic edifices is indicative of precipitation-driven pedogenic leaching pyroclastics deposits, which gives a new insight into the formation mechanism of compositional stratigraphy elsewhere on Mars and has crucial implications for Martian geologic history.

### 4.2. Implications for Martian Geologic History

Mars is in many ways a sedimentary planet (Grotzinger & Milliken, 2012; McLennan et al., 2019). However, where the sediments have been investigated in situ, there are many signs that point to volcaniclastic origins. These include fine-grained deposits of basaltic composition at Meridiani (Glotch et al., 2006), intensely weathered, soft rocks in Gusev Crater (Ruff et al., 2006, 2014), and sediments with a large amorphous component (Rampe et al., 2017) and high-temperature silica polymorphs in Gale Crater (Morris et al., 2016). Unlike the Earth, which contains mature sediments that have been chemically and physically processed over long periods of geologic activity and often great distances, it appears that sediments in some locations on Mars might be dominated by immature airfall volcaniclastic components.

It remains unclear how to reconcile the evidence for weathering observed with climate models, which generally do not predict sustained temperatures above freezing (e.g., Wordsworth et al., 2016). One piece of this puzzle is more easily solved if the weathered materials are widely composed of ash from explosive volcanoes. The amorphous, fragmented, mafic, porous, reactive ash deposits composed of particles with high specific surface area would have been much more susceptible to alteration in shorter times than nearly any other rock type (e.g., Gonnermann & Manga, 2007; Ugolini & Dahlgren, 2002).

Ancient, explosive volcanism could have significantly impacted the Noachian climate (Halevy & Head, 2014; Halevy et al., 2007; Johnson et al., 2008). The violent eruptions not only could have sent a large amount of ash to several kilometers height in the atmosphere, affecting climate, but also would have released large quantities of $H_2O$, $SO_x$, $CO_2$, $H_2$, $CH_4$, and other greenhouse gases into the atmosphere in a relatively short time period (e.g., Halevy & Head, 2014). There could therefore be a causal link between the volcanism that produces chemically reactive volcanic ash deposits and the triggers for climate excursions that drove weathering.

## 5. Conclusion

Compositional stratigraphy was found on the summits and flanks of volcanoes at high elevations in Thaumasia Planum, which provides compelling evidence for precipitation-driven weathering of pyroclastic deposits. This observation links widespread weathering sequences with explosive eruptions in early Martian history, both temporally and contextually. Considering that explosive volcanism might have been a widespread process on early Mars (Bandfield et al., 2013), volcaniclastic are likely a significant component of the Martian sedimentary record. The rapid alteration of these glassy, porous, and highly reactive materials is perhaps a critical puzzle piece to help to answer the climate conundrum of Mars' first billion years.

## Data Availability Statement

All data used in this paper are available in the NASA Planetary Data System (pds.jpl.nasa.gov).

**Acknowledgments**
The authors would like to thank Elizabeth Rampe and an anonymous reviewer for their thorough and insightful comments and suggestions during the review process that significantly improved the quality of the manuscript. This project was supported by the Research Grants Council General Research Fund grant number 17301718 to J. Michalski.

## References

Bandfield, J. L., Edwards, C. S., Montgomery, D. R., & Brand, B. D. (2013). The dual nature of the martian crust: Young lavas and old clastic materials. *Icarus*, *222*, 188–199.

Bishop, J. L., Dobrea, E. Z. N., McKeown, N. K., Parente, M., Ehlmann, B. L., Michalski, J. R., et al. (2008). Phyllosilicate diversity and past aqueous activity revealed at Mawrth Vallis, Mars. *Science*, *321*, 830–833.

Bishop, J., Madejová, J., Komadel, P., & Fröschl, H. (2002). The influence of structural Fe, Al and Mg on the infrared OH bands in spectra of dioctahedral smectites. *Clay Minerals*, *37*(4), 607–616.

Bishop, J. L., & Rampe, E. B. (2016). Evidence for a changing Martian climate from the mineralogy at Mawrth Vallis. *Earth and Planetary Science Letters*, *448*, 42–48.

Bishop, J. L., Rampe, E. B., Bish, D. L., Baker, L. L., Abidin, Z., Matsue, N., et al. (2013). Spectral and hydration properties of allophane and imogolite. *Clays and Clay Minerals*, *61*, 57–74.

Carter, J., Loizeau, D., Mangold, N., Poulet, F., & Bibring, J. P. (2015). Widespread surface weathering on early Mars: A case for a warmer and wetter climate. *Icarus*, *248*, 373–382.

Carter, J., Poulet, F., Bibring, J. P., Mangold, N., & Murchie, S. (2013). Hydrous minerals on Mars as seen by the CRISM and OMEGA imaging spectrometers: Updated global view. *Journal of Geophysical Research: Planets*, *118*, 831–858. https://doi.org/10.1029/2012JE004145

Christensen, P. R., Jakosky, B., Kieffer, H. H., Malin, M. C., McSween, H. Y., Nealson, K., et al. (2004). The Thermal Emission Imaging System (THEMIS) for the Mars 2001 Odyssey Mission. *Space Science Reviews*, *110*, 85–130.

Clark, R. N., King, T. V., Klejwa, M., Swayze, G. A., & Vergo, N. (1990). High spectral resolution reflectance spectroscopy of minerals. *Journal of Geophysical Research*, *95*(B8), 12653–12680. https://doi.org/10.1029/JB095iB08p12653

Clark, R. N., Swayze, G. A., Wise, R., Livo, E., Hoefen, T., Kokaly, R., et al. (2007). *USGS digital spectral library splib06a*, Denver, CO: U.S. Geological Survey Data Series 231.

Connerney, J. E., Acuna, M. H., Ness, N. F., Kletetschka, G., Mitchell, D. L., Lin, R. P., et al. (2005). Tectonic implications of Mars crustal magnetism. *Proceedings of the National Academy of Sciences*, *102*, 14970–14975.

Crown, D. A., & Greeley, R. (1993). Volcanic geology of Hadriaca-Patera and the Eastern Hellas Region of Mars. *Journal of Geophysical Research*, *98*(E2), 3431–3451. https://doi.org/10.1029/92JE02804

Cuadros, J., & Michalski, J. R. (2013). Investigation of Al-rich clays on Mars: Evidence for kaolinite-smectite mixed-layer versus mixture of end-member phases. *Icarus*, *222*, 296–306.

Dickson, J. L., Kerber, L. A., Fassett, C. I., & Ehlmann, B. L. (2018). A global, blended CTX mosaic of Mars with vectorized seam mapping: A new mosaicking pipeline using principles of non-destructive image editing. In *Presented at 49th Lunar Planet. Sci. Conf.* Abstract 2480.

Dohm, J., & Tanaka, K. (1999). Geology of the Thaumasia region, Mars: Plateau development, valley origins, and magmatic evolution. *Planetary and Space Science*, *47*(3–4), 411–431.

Dohm, J. M., Tanaka, K. L., Hare, T. M., Cartographer (2001). *Geological map of the Thaumasia region, Mars* (p. 2650). Flagstaff, AZ: U.S. Geological Survey Geologic Investigations Series I. Retrieved from https://pubs.usgs.gov/imap/i2650/

Ehlmann, B. L., Mustard, J. F., Murchie, S. L., Bibring, J. P., Meunier, A., Fraeman, A. A., et al. (2011). Subsurface water and clay mineral formation during the early history of Mars. *Nature*, *479*, 53–60.

Ehlmann, B. L., Mustard, J. F., Swayze, G. A., Clark, R. N., Bishop, J. L., Poulet, F., et al. (2009). Identification of hydrated silicate minerals on Mars using MRO-CRISM: Geologic context near Nili Fossae and implications for aqueous alteration. *Journal of Geophysical Research*, *114*, E00D08. https://doi.org/10.1029/2009JE003339

Ehlmann, B. L., Swayze, G. A., Milliken, R. E., Mustard, J. F., Clark, R. N., Murchie, S. L., et al. (2016). Discovery of alunite in Cross crater, Terra Sirenum, Mars: Evidence for acidic, sulfurous waters. *American Mineralogist*, *101*, 1527–1542.

El-Maarry, M. R., Watters, W., McKeown, N. K., Carter, J., Dobrea, N. E., Bishop, J. L., et al. (2014). Potential desiccation cracks on Mars: A synthesis from modeling, analogue-field studies, and global observations. *Icarus*, *241*, 248–268.

Fergason, R. L., Christensen, P. R., & Kieffer, H. H. (2006). High-resolution thermal inertia derived from the Thermal Emission Imaging System (THEMIS): Thermal model and applications. *Journal of Geophysical Research*, *111*, E12004. https://doi.org/10.1029/2006JE002735

Gaudin, A., Dehouck, E., & Mangold, N. (2011). Evidence for weathering on early Mars from a comparison with terrestrial weathering profiles. *Icarus*, *216*, 257–268.

Glotch, T. D., Bandfield, J. L., Christensen, P. R., Calvin, W. M., McLennan, S. M., Clark, B. C., et al. (2006). Mineralogy of the light-toned outcrop at Meridiani Planum as seen by the Miniature Thermal Emission Spectrometer and implications for its formation. *Journal of Geophysical Research*, *111*, E12S03. https://doi.org/10.1029/2005JE002672

Gonnermann, H. M., & Manga, M. (2007). The fluid mechanics inside a volcano. *Annual Review of Fluid Mechanics*, *39*, 321–356.

Grant, J. A., & Schultz, P. H. (1990). Gradational epochs on Mars: Evidence from west-northwest of Isidis Basin and Electris. *Icarus*, *84*(1), 166–195.

Grotzinger, J. P., & Milliken, R. E. (2012). The sedimentary rock record of Mars: Distribution, origins, and global stratigraphy. *Sedimentary Geology of Mars*, *102*, 1–48.

Gulick, V. C., & Baker, V. R. (1990). Origin and evolution of valleys on Martian volcanoes. *Journal of Geophysical Research*, *95*(B9), 14325–14344. https://doi.org/10.1029/JB095iB09p14325

Gustafson, J. O., Bell, J. F., III, Gaddis, L. R., Hawke, B. R., & Giguere, T. A. (2012). Characterization of previously unidentified lunar pyroclastic deposits using Lunar Reconnaissance Orbiter Camera data. *Journal of Geophysical Research*, *117*, E00H25. https://doi.org/10.1029/2011JE003893

Halevy, I., & Head, J. W., III (2014). Episodic warming of early Mars by punctuated volcanism. *Nature Geoscience*, *7*, 865.

Halevy, I., Zuber, M. T., & Schrag, D. P. (2007). A sulfur dioxide climate feedback on early Mars. *Science*, *318*, 1903–1907.

Johnson, S. S., Mischna, M. A., Grove, T. L., & Zuber, M. T. (2008). Sulfur-induced greenhouse warming on early Mars. *Journal of Geophysical Research*, *113*, E08005. https://doi.org/10.1029/2007JE002962

Kerber, L., Head, J. W., Madeleine, J.-B., Forget, F., & Wilson, L. (2012). The dispersal of pyroclasts from ancient explosive volcanoes on Mars: Implications for the friable layered deposits. *Icarus*, *219*, 358–381.

Kremer, C. H., Mustard, J. F., & Bramble, M. S. (2019). A widespread olivine-rich ash deposit on Mars. *Geology*, *47*, 677–681.

Le Deit, L., Flahaut, J., Quantin, C., Hauber, E., Mege, D., Bourgeois, O., et al. (2012). Extensive surface pedogenic alteration of the Martian Noachian crust suggested by plateau phyllosilicates around Valles Marineris. *Journal of Geophysical Research*, *117*, E00J05. https://doi.org/10.1029/2011JE003983

Lillis, R. J., Frey, H. V., Manga, M., Mitchell, D. L., Lin, R. P., Acuña, M. H., et al. (2008). An improved crustal magnetic field map of Mars from electron reflectometry: Highland volcano magmatic history and the end of the Martian dynamo. *Icarus*, *194*, 575–596.

Malin, M. C., Bell, J. F., Cantor, B. A., Caplinger, M. A., Calvin, W. M., Clancy, R. T., et al. (2007). Context Camera Investigation on board the Mars Reconnaissance Orbiter. *Journal of Geophysical Research*, *112*, E05S04. https://doi.org/10.1029/2006JE002808

McEwen, A. S., Eliason, E. M., Bergstrom, J. W., Bridges, N. T., Hansen, C. J., Delamere, W. A., et al. (2007). Mars Reconnaissance Orbiter's High Resolution Imaging Science Experiment (HiRISE). *Journal of Geophysical Research*, *112*, E05S02. https://doi.org/10.1029/2005JE002605

McKeown, N., Bishop, J. L., Cuadros, J., Hillier, S., Amador, E., Makarewicz, H. D., et al. (2011). Interpretation of reflectance spectra of clay mineral-silica mixtures: Implications for Martian clay mineralogy at Mawrth Vallis. *Clays and Clay Minerals*, *59*, 400–415.

McKeown, N. K., Bishop, J. L., Dobrea, E. Z. N., Ehlmann, B. L., Parente, M., Mustard, J. F., et al. (2009). Characterization of phyllosilicates observed in the central Mawrth Vallis region, Mars, their potential formational processes, and implications for past climate. *Journal of Geophysical Research*, *114*, E00D10. https://doi.org/10.1029/2008JE003301

McLennan, S. M., Grotzinger, J. P., Hurowitz, J. A., & Tosca, N. J. (2019). The Sedimentary Cycle on Early Mars. *Annual Review of Earth and Planetary Sciences*, *47*, 91–118.

Mellon, M. T., Jakosky, B. M., Kieffer, H. H., & Christensen, P. R. (2000). High-resolution thermal inertia mapping from the Mars Global Surveyor Thermal Emission Spectrometer. *Icarus*, *148*(2), 437–455.

Michalski, J. R., & Bleacher, J. E. (2013). Supervolcanoes within an ancient volcanic province in Arabia Terra, Mars. *Nature*, *502*, 47–52.

Michalski, J. R., Cuadros, J., Bishop, J. L., Dyar, M. D., Dekov, V., & Fiore, S. (2015). Constraints on the crystal-chemistry of Fe/Mg-rich smectitic clays on Mars and links to global alteration trends. *Earth and Planetary Science Letters*, *427*, 215–225.

Michalski, J. R., Niles, P. B., Cuadros, J., & Baldridge, A. M. (2013). Multiple working hypotheses for the formation of compositional stratigraphy on Mars: Insights from the Mawrth Vallis region. *Icarus*, *226*, 816–840.

Moore, J. M. (1990). Nature of the mantling deposit in the heavily cratered terrain of northeastern Arabia, Mars. *Journal of Geophysical Research*, *95*(B9), 14279–14289. https://doi.org/10.1029/JB095iB09p14279

Morris, R. V., Vaniman, D. T., Blake, D. F., Gellert, R., Chipera, S. J., Rampe, E. B., et al. (2016). Silicic volcanism on Mars evidenced by tridymite in high-SiO2 sedimentary rock at Gale crater. *Proceedings of the National Academy of Sciences*, *113*, 7071–7076.

Murchie, S., Arvidson, R., Bedini, P., Beisser, K., Bibring, J. P., Bishop, J., et al. (2007). Compact reconnaissance Imaging Spectrometer for Mars (CRISM) on Mars Reconnaissance Orbiter (MRO). *Journal of Geophysical Research*, *112*, E00D07. https://doi.org/10.1029/2006JE002682

Murchie, S. L., Mustard, J. F., Ehlmann, B. L., Milliken, R. E., Bishop, J. L., McKeown, N. K., et al. (2009). A synthesis of Martian aqueous mineralogy after 1 Mars year of observations from the Mars Reconnaissance Orbiter. *Journal of Geophysical Research*, *114*, 0–6. https://doi.org/10.1029/2009JE003342

Neukum, G., Jaumann, R., Hoffmann, H., Hauber, E., Head, J. W., Basilevsky, A. T., et al. (2004). Recent and episodic volcanic and glacial activity on Mars revealed by the High Resolution Stereo Camera. *Nature*, *432*, 971–979.

Noe Dobrea, E. Z., Bishop, J., McKeown, N., Fu, R., Rossi, C., Michalski, J., et al. (2010). Mineralogy and stratigraphy of phyllosilicate-bearing and dark mantling units in the greater Mawrth Vallis/west Arabia Terra area: Constraints on geological origin. *Journal of Geophysical Research*, *115*, E00D19. https://doi.org/10.1029/2009JE003351

Parfitt, R. L. (2009). Allophane and imogolite: role in soil biogeochemical processes. *Clay Minerals*, *44*, 135–155.

Pelkey, S. M., Mustard, J. F., Murchie, S., Clancy, R. T., Wolff, M., Smith, M., et al. (2007). CRISM multispectral summary products: Parameterizing mineral diversity on Mars from reflectance. *Journal of Geophysical Research*, *112*, E08S14. https://doi.org/10.1029/2006JE002831

Rampe, E. B., Ming, D. W., Blake, D. F., Bristow, T. F., Chipera, S. J., Grotzinger, J. P., et al. (2017). Mineralogy of an ancient lacustrine mudstone succession from the Murray formation, Gale crater, Mars. *Earth and Planetary Science Letters*, *471*, 172–185.

Robock, A. (2000). Volcanic eruptions and climate. *Reviews of Geophysics*, *38*(2), 191–219. https://doi.org/10.1029/1998RG000054

Rogers, A. D., Warner, N. H., Golombek, M. P., Head, J. W., III, & Cowart, J. C. (2018). Areally extensive surface bedrock exposures on Mars: Many are clastic rocks, not lavas. *Geophysical Research Letters*, *45*, 1767–1777. https://doi.org/10.1002/2018GL077030

Ruff, S. W., Christensen, P. R., Blaney, D. L., Farrand, W. H., Johnson, J. R., Michalski, J. R., et al. (2006). The rocks of Gusev Crater as viewed by the Mini-TES instrument. *Journal of Geophysical Research*, *111*, E12S18. https://doi.org/10.1029/2006JE002747

Ruff, S. W., Niles, P. B., Alfano, F., & Clarke, A. B. (2014). Evidence for a Noachian-aged ephemeral lake in Gusev crater, Mars. *Geology*, *42*, 359–362.

Smith, D. E., Zuber, M. T., Frey, H. V., Garvin, J. B., Head, J. W., Muhleman, D. O., et al. (2001). Mars Orbiter Laser Altimeter: Experiment summary after the first year of global mapping of Mars. *Journal of Geophysical Research*, *106*(E10), 23689–23722. https://doi.org/10.1029/2000JE001364

Tanaka, K. L., Skinner, J. A., Dohm, J. M., Irwin, R. P., Kolb, E. J., Fortezzo, C. M., et al. (2014). *Geologic map of Mars* (p. 43). Flagstaff, AZ: U.S. Geological Survey Scientific Investigations Map. 3292. Retrieved from https://dx.doi.org/10.3133/sim3292

Thomas, R. J., Rothery, D. A., Conway, S. J., & Anand, M. (2014). Mechanisms of explosive volcanism on Mercury: Implications from its global distribution and morphology. *Journal of Geophysical Research: Planets*, *119*, 2239–2254. https://doi.org/10.1002/2014JE004692

Ugolini, F. C., & Dahlgren, R. A. (2002). Soil development in volcanic ash. *Global Environmental Research-English Edition*, *6*(2), 69–82.

Viviano-Beck, C. E., Seelos, F. P., Murchie, S. L., Kahn, E. G., Seelos, K. D., Taylor, H. W., et al. (2014). Revised CRISM spectral parameters and summary products based on the currently detected mineral diversity on Mars. *Journal of Geophysical Research: Planets*, *119*, 1403–1431. https://doi.org/10.1002/2014JE004627

Wada, S. I., & Wada, K. (1977). Density and structure of allophane. *Clay Minerals*, *12*(4), 289–298.

Wilson, L., & Head, J. W., III (1994). Mars: Review and analysis of volcanic eruption theory and relationships to observed landforms. *Reviews of Geophysics*, *32*(3), 221–263. https://doi.org/10.1029/94RG01113

Wordsworth, R. D. (2016). The climate of early Mars. *Annual Review of Earth and Planetary Sciences*, *44*, 381–408.

Wray, J. J., Ehlmann, B. L., Squyres, S. W., Mustard, J. F., & Kirk, R. L. (2008). Compositional stratigraphy of clay-bearing layered deposits at Mawrth Vallis, Mars. *Geophysical Research Letters*, *35*, L12202. https://doi.org/10.1029/2008GL034385

Xiao, L., Huang, J., Christensen, P. R., Greeley, R., Williams, D. A., Zhao, J., et al. (2012). Ancient volcanism and its implication for thermal evolution of Mars. *Earth and Planetary Science Letters*, *323–324*, 9–18.

## References From the Supporting Information

Fassett, C. I., & Head, J. W., III. (2007). Layered mantling deposits in northeast Arabia Terra, Mars: Noachian-Hesperian sedimentation, erosion, and terrain inversion. *Journal of Geophysical Research*, *112*, E08002. https://doi.org/10.1029/2006JE002875

Greeley, R., & Crown, D. A. (1990). Volcanic geology of Tyrrhena Patera, Mars. *Journal of Geophysical Research*, *95*(B5), 7133–7149. https://doi.org/10.1029/JB095iB05p07133

Head, J. W., & Wilson, L. (1998). Tharsis Montes as stratovolcanoes?: 3. Lines of evidence for explosive volcanism in edifice construction. *Lunar and Planetary Science*, *29*(1124).

Hynek, B. M., Phillips, R. J., & Arvidson, R. E. (2003). Explosive volcanism in the Tharsis region: Global evidence in the Martian geologic record. *Journal of Geophysical Research*, *108*(E9), 5111. https://doi.org/10.1029/2003JE002062

Kerber, L., Michalski, J., Bleacher, J., & Forget, F. (2013). Ash sources in Arabia Terra? Implications for the Arabia Deposits, (pp. 2290). In *Proceedings of the Lunar and Planetary Science Conference*.

Keszthelyi, L., McEwen, A. S., & Thordarson, T. (2000). Terrestrial analogs and thermal models for Martian flood lavas. *Journal of Geophysical Research*, *105*(E6), 15027–15049. https://doi.org/10.1029/1999JE001191

Mouginis-Mark, P. J. (2002). Prodigious ash deposits near the summit of Arsia Mons volcano, Mars. *Geophysical Research Letters*, *29*(16), 15–11–15– 14, 1768. https://doi.org/10.1029/2002GL015296

Mouginis-Mark, P. J., Wilson, L., & Head, J. W., III (1982). Explosive volcanism on Hecates Tholus, Mars: Investigation of eruption conditions. *Journal of Geophysical Research*, *87*(B12), 9890–9904. https://doi.org/10.1029/JB087iB12p09890

Robinson, M. S., Mouginismark, P. J., Zimbelman, J. R., Wu, S. S., Ablin, K. K., & Howingtonkraus, A. E. (1993). Chronology, eruption duration, and atmospheric contribution of the Martian Volcano Apollinaris-Patera. *Icarus*, *104*, 301–323.

Williams, D. A., Greeley, R., Manfredi, L., Raitala, J., Neukum, G., & Team, H. C.-I. (2010). The Circum-Hellas Volcanic Province, Mars: Assessment of wrinkle-ridged plains. *Earth and Planetary Science Letters*, *294*, 492–505.

Wilson, L., & Mouginis-Mark, P. J. (1987). Volcanic input to the atmosphere from Alba Patera on Mars. *Nature*, *330*(6146), 354–357.